

PACS numbers: 61.72.Uj, 78.30.FS, 78.55.Et

SYNTHESIS AND CHARACTERIZATION OF ZnO NANOPARTICLES

*N. Singh*¹, *R.M. Mehra*², *A. Kapoor*¹

¹ Department of Electronic Science, University of Delhi south Campus,
NewDelhi-110021, India
E-mail: Singhneetu1985@gmail.com

² School of Engineering and Technology, Sharda University,
Greater Noida-201306 Uttar Pradesh, India

In this paper, we report the comparison between ZnO nanoparticles prepared via two different routes; i) via sol-gel route and ii) by solid state reaction method. It was found that when prepared under the same ambient conditions viz temperature, pressure etc. and keeping all the parameters same viz precursors, molarity, solvent etc; the nanoparticles prepared via Sol-gel route were highly crystalline and had smaller crystallite size (~ 24 nm) as compared to the one prepared by Solid state reaction method (~ 37 nm). The crystallinity and the crystallite size were examined by XRD and TEM. Variation in the bandgap as a function of size of the particles was determined using the absorption spectra obtained by UV-Vis-NIR spectrophotometer. Photoluminescence (PL) was also recorded in the visible region for the two types of particles and results have been analysed.

Keywords: SYNTHESIS, ZnO, NANOPARTICLES.

(Received 04 February 2011, in final form 17 March 2011)

1. INTRODUCTION

Zinc Oxide is a member of II-VI semiconducting compounds and occurs naturally as the mineral zincite. It is a hexagonal wurtzite type crystal exhibiting anisotropy. ZnO is a well-known n-type semiconductor and has got a wide band gap of 3.3 eV at 300 K. Some of its important properties are listed in Table 1 [10-16]. ZnO is considered a good candidate for transparent conducting electrodes in solar cells because it is transparent to the visible light [1]. It is also considered as a prime candidate for UV and blue light-emitting devices such as blue LED and Lasers due to its large exciton binding energy of 60 meV [2, 3]. Due to such large exciton binding energy, the excitons remain dominant in optical processes even at room temperature. Due to its vast industrial applications such as electro-photography, electroluminescence phosphorus, pigment in paints, flux in ceramic glazes, filler for rubber products, coatings for paper, sunscreens, medicines and cosmetics, ZnO is attracting considerable attention in powder as well as thin film form. Its resistance to radiation damages also makes it useful for space applications. The fabrication of ZnO nanostructures have attracted intensive research interests [4-5] as these materials have found uses as transparent conducting oxides (TCO) [8-9]. Since it is the hardest of the II-VI family of semiconductors with a large shear modulus, its performance is not degraded as easily as the other compounds through the

appearance of defects. Since Zinc, the main constituent is cheap, non-toxic and abundant, ZnO has become commercially viable.

In the present work, we have synthesized ZnO nanoparticles via two different routes (sol-gel route and solid state reaction method) and tried to analyze the two on the basis of their crystallinity, crystallite size, bandgap and structural properties. X-ray diffraction (XRD) is used to calculate crystallite size. Variation in the bandgap as a function of size of the particles is determined using the absorption spectra obtained by UV-Vis-NIR spectrophotometer. Photoluminescence (PL) is also recorded in the visible region. Transmission electron micrograph (TEM) and Scanning electron micrograph (SEM) images are shown to clearly see the particle size and grain size respectively.

Table 1 – Properties of zinc oxide

Properties	Values
Crystal structure	Rock salt, Zinc blende and Wurtzite
Energy Bandgap, eV	3.2-3.3
Electron Mobility, $\text{cm}^2\text{Vs}^{-1}$	2.5-300 (Bulk ZnO), 1000 (Single nanowire)
Exciton Binding Energy, meV	60
Density, g/cm^3	5.606
Refractive Index	2.0041
Electron Effective Mass (m_e)	0.26
Relative Dielectric Constant	8.5
Melting point, °C	1975
Boiling point, °C	2360
Electron Diffusion Coefficient, cm^2s^{-1}	5.2 (Bulk ZnO), 1.7×10^{-7} (Particulate Film)

2. EXPERIMENTAL

2.1 Sol-gel route

All the reagents used were of analytical grade and no further purification was done before use. ZnO nanopowder was prepared by dissolving 0.2M Zinc acetate dihydrate [$\text{Zn}(\text{CH}_3\text{COO})_2 \cdot 2\text{H}_2\text{O}$] in methanol at room temperature and then mixing this solution ultrasonically at 25 °C for 2h. Clear and transparent sol with no precipitate and turbidity was obtained. 0.02 M of NaOH was then added in the sol and stirred ultrasonically for 60 min. The sol was kept undisturbed till white precipitates were seen in the sol. After precipitation, the precipitates were filtered and washed with the excess methanol to remove starting material. Precipitates were then dried at 80 °C for 15 min on hot plate.

2.2 Solid state reaction method

The chemical reagents used in this work were Zinc acetate dihydrate [$\text{Zn}(\text{CH}_3\text{COO})_2 \cdot 2\text{H}_2\text{O}$] and NaOH powders of analytical grade purity. In solid-state reaction method, 0.2 M of Zinc acetate dihydrate [$\text{Zn}(\text{CH}_3\text{COO})_2 \cdot 2\text{H}_2\text{O}$] was ground for 10 min and then mixed with 0.02 M of NaOH. After the mixture was ground for 30 min, the product was washed many times with

deionized water and methanol to remove the by-products. The final product was then filtered and dried into solid powders at 80 °C for 15 min on hot plate.

The XRD measurements were carried out using Bruker AXS-D8 discover diffractometer. The absorbance of the powder in the visible region was measured using Shimadzu UV-VIS-NIR spectrophotometer (solidspec-3700). PL measurements were carried out using Shimadzu RF-5301 PC spectrofluorophotometer under 325 nm excitation wavelength. The crystallite size calculated from the XRD measurements was confirmed by TEM Morgagni-268D FEI.

3. RESULTS AND DISCUSSION

The XRD patterns of the nanoparticles obtained by sol-gel route and solid state reaction method are shown in Fig. 1 and 2 respectively. The nanoparticles synthesized by both methods showed crystalline nature with 2θ peaks lying at 31.750° <100>, 34.440° <002>, 36.252° <101>, 47.543° <102>, 56.555° <110>, 62.870° <103>, 66.388° <200>, 67.917° <112>, 69.057° <201>, 72.610° <004>, 76.95° <202>, 81.405° <104>, and 89.630° <203>. The preferred orientation corresponding to the plane <101> is observed in both the samples. These peak positions coincide with JCPDS card no. 36-1451 for ZnO powder. Crystallite size was obtained by Debye-Scherrer formula given by equation

$$D = \frac{0.94 \lambda}{\beta \cos \theta}, \quad (1)$$

where D is the crystallite size, 0.94 is the particle shape factor which depends on the shape of the particles, λ is the CuK_α radiations (1.54 Å), β is full width at half maximum (FWHM) of the selected diffraction peak corresponding to 101 plane and θ is the Bragg angle obtained from 2θ value corresponding to maximum intensity peak in XRD pattern. The crystallite size obtained using this formula is 23.585 nm for sol-gel derived particles and 37.344 nm in case of solid state reaction method derived particles.

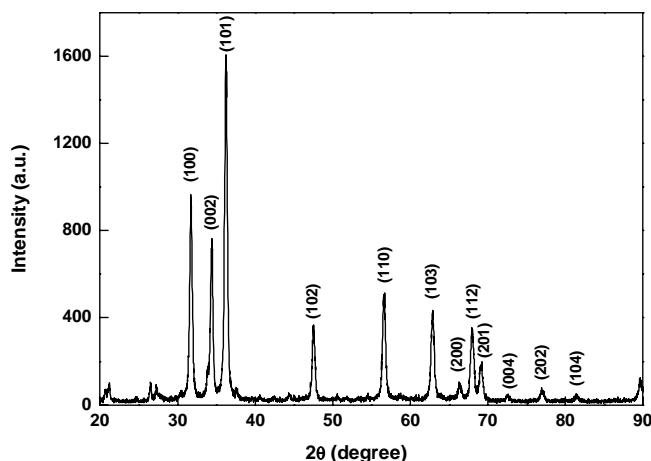


Fig. 1 – XRD pattern of ZnO nanoparticles synthesized via sol-gel route

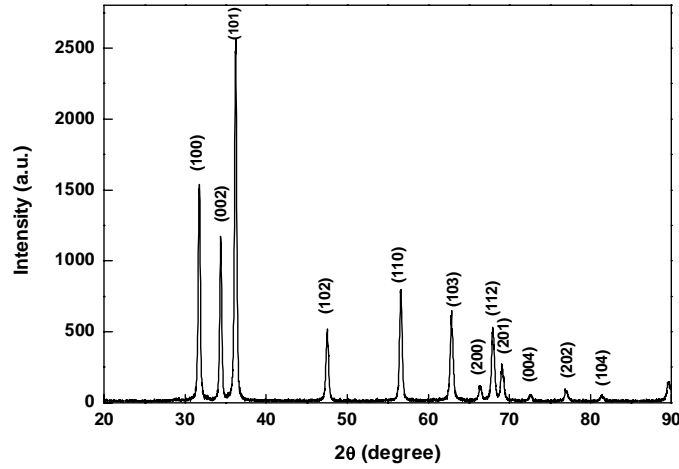


Fig. 2 – XRD pattern of ZnO nanoparticles synthesized via solid state reaction method

The absorbance curve of the sol-gel derived nanoparticles in the visible region is shown in Fig. 3(a). The graph shows that ZnO does not absorb light in the visible region. This result is in accordance with the bandgap value of the bulk ZnO (3.37 eV) according to which ZnO absorbs light in ultra violet (UV) range. Band gap energy is calculated using Tauc's plot Fig. 3b which comes out to be 3.23 eV in case of sol-gel derived nanoparticles. Tauc's equation (2) is given by [17]

$$\alpha h\nu = A(h\nu - E_g)^n, \quad (2)$$

where α is the absorption coefficient, $h\nu$ is the photon energy, A is the constant, E_g is the bandgap energy of the sample. The value of n is 1/2 or 2 depending upon whether the transition from valence band to conduction band is direct or indirect. The value is 1/2 in case of direct transition and 2 in case of indirect transition. Since ZnO has a direct band structure, the value of n is 1/2 in this case. So, the equation takes the form

$$(\alpha h\nu)^2 = B(h\nu - E_g), \quad (3)$$

where, B is a constant related effective masses of charge carriers associated with valence and conduction bands. Intersection of the slope of $(\alpha h\nu)^2$ vs $h\nu$ curve provides bandgap energy of the samples. According to the experimentally calculated bandgap, the synthesized ZnO nanoparticles should absorb light below 383 nm and absorbance graph is in agreement with this.

The absorbance curve of the solid state reaction derived nanoparticles in the visible region is shown in Fig. 4a. Tauc's plot is shown in Fig. 4b. The band gap energy comes out to be 3.15 eV from the Tauc's plot. According to the experimentally calculated bandgap, the synthesized ZnO nanoparticles should absorb light below 393 nm in this case and absorbance graph shows this thing. The band gap values validates our crystallite size results according to which smaller crystallite size should have larger band gap (23.585 nm, 3.23 eV for sol-gel derived nanoparticles) and large crystallite size should have smaller band gap (37.344 nm, 3.15 eV for solid state reaction derived nanoparticles).

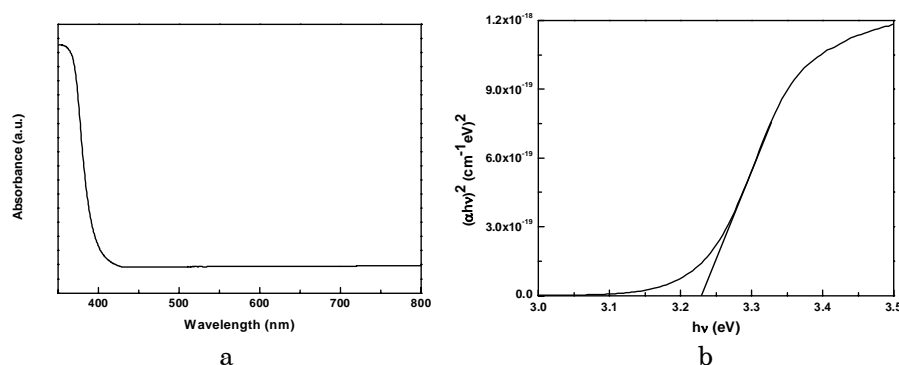


Fig. 3 – Absorbance of sol-gel derived nanoparticles visible range (a) Tauc's plot of sol-gel derived nanoparticles (b)

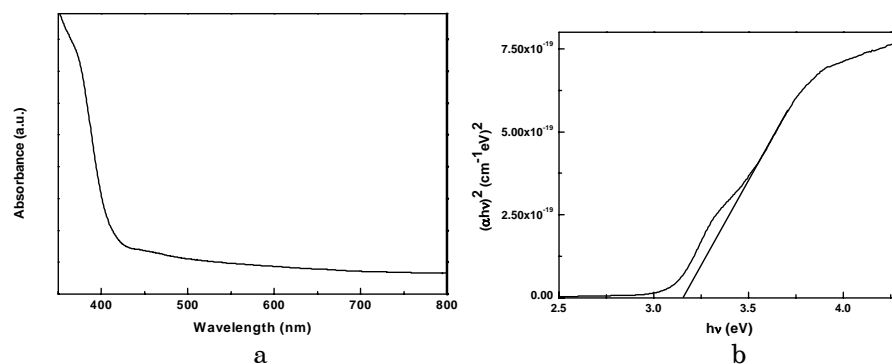


Fig. 4 – Absorbance of solid state reaction derived nanoparticles in visible rang (a) Tauc's plot of solid state reaction derived nanoparticles (b)

Photoluminescence (PL) spectra of the nanoparticles obtained by both the processes are shown in Fig. 5. The first peak in PL spectra corresponds to band to band transition and the spectra between 420-500 nm are showing blue luminescence. ZnO nanoparticles prepared via solid state reaction method show high luminescence than sol-gel derived nanoparticles. This could be due to the chemical instability caused during the fabrication process. As can be seen from the PL spectrum of sol-gel derived nanoparticles, the intensity peak is observed at 388.6 nm. If we calculate the band gap value from this wavelength, it comes out to be 3.2 eV. The PL intensity peak in case of solid state reaction derived nanoparticles is observed at 391.5 nm. From this value, band gap comes out to be 3.16 eV. The band gap energies calculated using PL spectra are approximately same as the ones calculated using Tauc's plot.

TEM images of sol-gel derived nanoparticles are shown in Fig. 6a. Clear hexagonal structures can be seen in the Fig. 6c having diameter ~ 23 nm. Selected area diffraction is shown in Fig. 6b which clearly indicates that the ZnO nanoparticles are highly crystalline in nature.

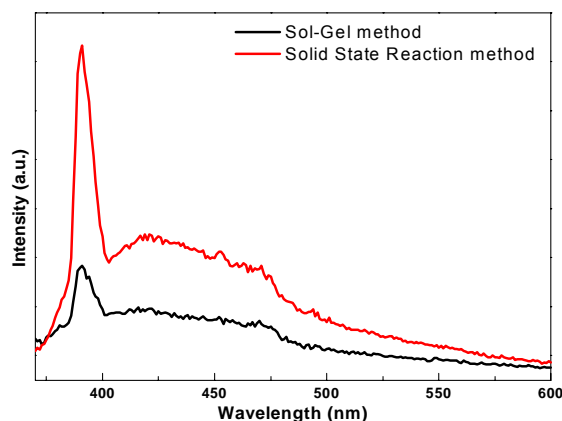


Fig. 5 – Photoluminescence peak of ZnO nanoparticles obtained via different method

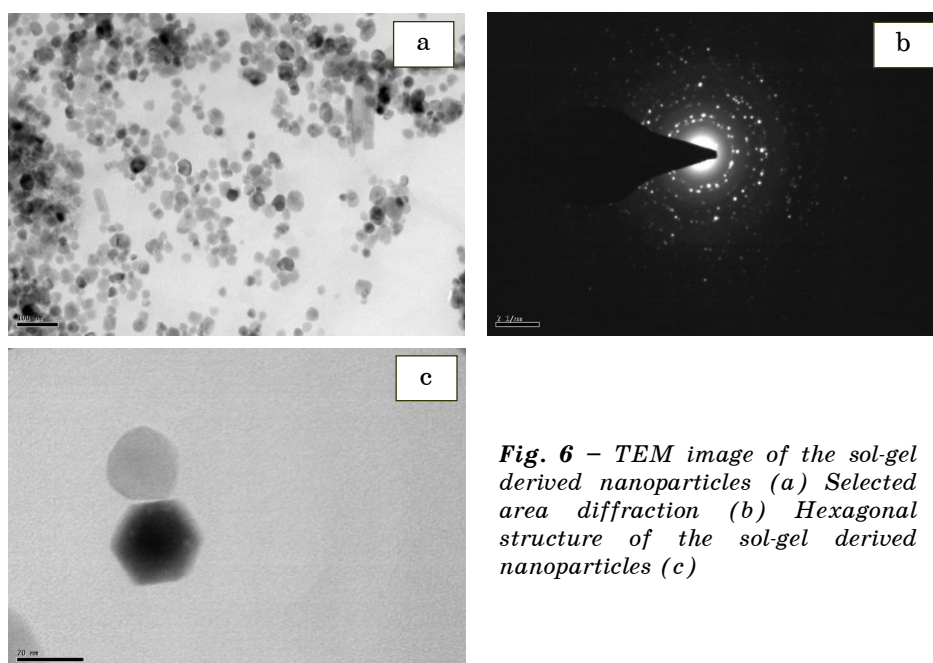


Fig. 6 – TEM image of the sol-gel derived nanoparticles (a) Selected area diffraction (b) Hexagonal structure of the sol-gel derived nanoparticles (c)

TEM image and selected area diffraction pattern of the solid state reaction derived nanoparticles are shown in Fig. 7a and 7b respectively. Selected area diffraction pattern of the nanoparticles indicates that the ZnO nanoparticles prepared via solid state reaction method are crystalline in nature. However the diffraction rings in this case are not properly aligned as in the case of sol-gel derived nanoparticles. No clear hexagonal structures can be seen in the TEM image. Nanoparticles obtained in this case are adhering to one another. Agglomeration of nanoparticles is more in this case than the former one. As can be seen from the TEM image that the average particle size is ~ 37 nm which is in agreement with the crystallite size obtained from XRD.

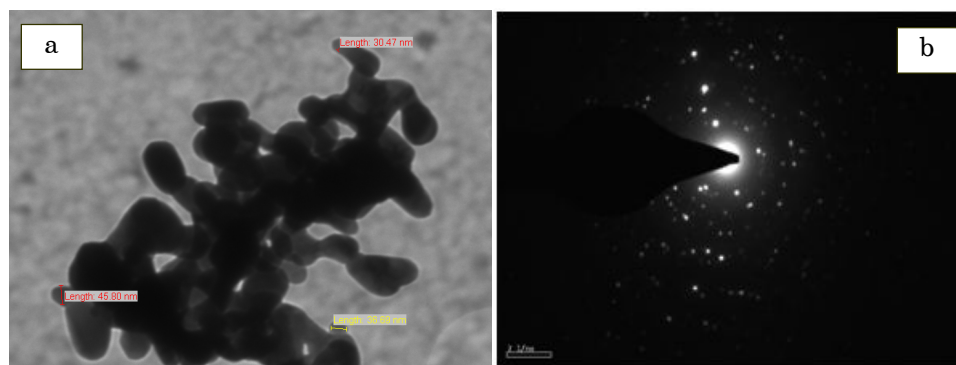


Fig. 7 – TEM image (a) Selected area diffraction of solid state reaction derived ZnO nanoparticles (b)

SEM images of the nanoparticles prepared via both the routes are shown in Fig. 8. Fig. 8a shows the SEM image of sol-gel derived nanoparticles. Clear nanostructures can be seen having grain size of ~ 70 nm. The crystallite size as observed from TEM in this case is ~ 24 nm. This shows that one grain in sol-gel derived nanoparticles is approximately equal to three crystallites. So it is clear that the nanoparticles seen by SEM image consist of a number of crystallites which are seen by TEM image. SEM image of nanoparticles prepared by solid state reaction method is shown in Fig. 8b. Grain size in this case is ~ 200 nm. Crystallite size as seen from TEM image is ~ 37 nm in this case. This shows that one grain in solid state reaction derived nanoparticles consists of approximately five crystallites. XRD results are confirmed by the combined study of these SEM and TEM images.

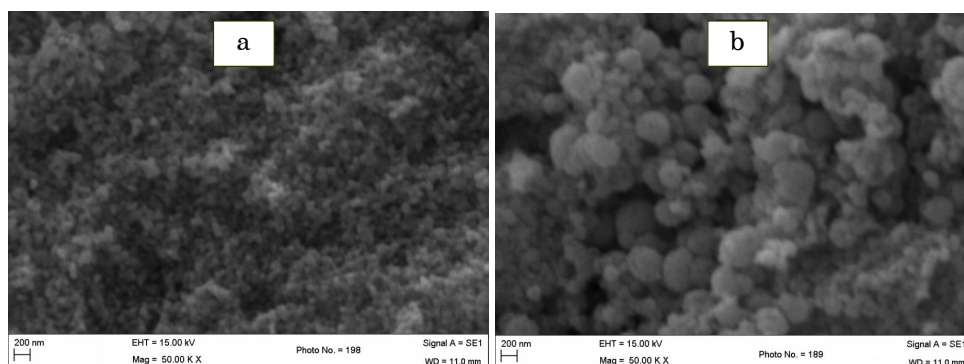


Fig. 8 – Scanning electron micrographs via sol-gel route (a) via solid state reaction method (b)

4. CONCLUSION

ZnO nanoparticles were prepared via sol-gel and solid state reaction methods. The ZnO nanoparticles prepared via sol-gel route were highly crystalline and had smaller crystallite size (~ 24 nm) as compared to the one prepared by Solid state reaction method (~ 37 nm). The bandgap of the synthesised nanoparticles was found to be size dependent. Photoluminescence (PL) study confirms the results obtained by XRD and TEM.

ACKNOWLEDGMENTS

This work is done under the DST-JSPS sponsored project DST/INT/JSPS/PROJ/10. Financial support by University Grant Commission, India in the form of JRF is also acknowledged. The authors are thankful to University Science Instrumentation Centre (USIC) for providing XRD facility, All India Institute of Medical Sciences (AIIMS) for providing TEM facility and Prof. P.K. Bhatnagar from Department of Electronic Science, Delhi University for providing PL facility.

REFERENCES

1. D.R. Lide, *Hand Book of Chemistry and Physics*, 71st ed. (CRC, Boca Raton, FL: 1991)
2. A. Ohtomo, M.Kawasaki, I. Ohkubo, H. Koinuma, T. Yasuda, Y. Segawa, *Appl. Phys. Lett.* **75**, 980 (1999).
3. Z.K. Tang, G.K.L. Wong, P. Yu, M. Kawasaki, A. Ohtomo, H. Koinuma, Y. Segawa, *Appl. Phys. Lett.* **72**, 3270 (1998).
4. Y.W. Wang, L.D. Zhang, G.Z. Wang, X.S. Peng, Z.Q. Chu, C.H. Liang, *J. Crystal Growth* **234**, 171 (2002).
5. M.H. Huang, S. Mao, H. Feick, H. Yen, Y. Wu, H. Kind, E. Weber, R. Russo, P. Yang, *Science* **292** 1897 (2001).
6. W. Zhu, C. Bower, O. Zhou, G. Kochanski, S. Jin, *Appl. Phys. Lett.* **75**, 873 (1999).
7. C.J. Lee, S.C. Lyu, Y. Zhang, H. Ruh, H.J. Lee, *Appl. Phys. Lett.* **81**, 3648 (2002).
8. J.W. Bae, S.W. Lee, K.H. Song, J.I. Park, J.J. Park, Y.W. Ko, G.Y. Yeom, *Jpn. J. Appl. Phys.* **38**, 2917 (1999).
9. G.K. Paul, S. Bandopadhyya, S.K. Sen, *phys. stat. solid a* **191** No2, 509 (2002).
10. Ozgur, Y.I. Alivov, C. Liu, A. Teke, M.A. Reshchikov, S. Dogan, V. Avrutin, S.J. Cho, H. Morkoc, *J. Appl. Phys.* **98**, 41301 (2005).
11. H. Tang, K. Prasad, R. Sanijines, P.E. Schmid, F. Levy, *J. Appl. Phys.* **75**, 2042 (1994).
12. G. Oskam, Z.S. Hu, R.L. Penn, N. Pesika, P.C. Searson, *Phys. Rev. E* **66**, 11403 (2002).
13. H.S. Bae, M.H. Yoon, J.H. Kim, S. Im, *Appl. Phys. Lett.* **83**, 5313 (2003).
14. K. Keis, A. Roos, *Opt. Mater.* **20**, 35 (2002).
15. V. Noack, H. Weller, A. Evchmuller, *J. Phys. Chem. B* **106**, 8514 (2002).
16. J.J. Wu, G.R. Chen, C.C. Lu, W.T. Wu, J.S. Chen, *Nanotechnology* **19**, 105702 (2008).
17. A.B. Kashyout, M. Soliman, M.El Gamal, M. Fathy, *Mat. Chem. Phys.* **90**, 230 (2005).